A Review of the Fatigue Behaviour of Laser Powder Bed Fusion Ti6Al4V

Tumelo Moloi[1], Thywill Cephas Dzogbewu[1], Maina Maringa[1], Amos Muiruri[2]

[1]*Department of Mechanical and Mechatronics Engineering, Central University of Technology, Free State, Private Bag X20539, Bloemfontein 9300, South Africa*
[2]*Department of Mechanical Engineering, Murang'a University of Technology, P.O. Box 75-10200, Murang'a, Kenya*
Email: moloitd7@gmail.com

Abstract: Fatigue in metals has been recognized since the early 1800s, after several cases of fatigue failure were reported. It is described as a material's deterioration brought on by repeated loading that causes progressive, localised structural damage. Fatigue is a problem that affects engineering components that are under the action of cyclic stresses. In these components fatigue failure always occurs at significantly much lower stresses than the yield strength of material. Unlike in the early days of failure, the causes of failure in engineering structures have been studied thoroughly and are nowadays well known. The theory of fatigue allows engineers to design components with the aim of minimizing the possibility of failure. However, it is not possible to guarantee that fatigue failure will not occur, and therefore, the recourse to damage tolerance approach in design for cyclically loaded components. The last few years have seen a pickup of the various additive manufacturing (AM) technologies. This is because AM leads to shorter manufacturing times and is capable of producing parts with complicated geometries and assemblies of interconnected parts. Unlike traditional manufacturing methods, AM does not require post-machining processes thus leading to minimal wastage of material. The microstructures of additively manufactured parts are finer than those of traditional methods, and the strength is higher on the AM parts, but ductility is lower. As in traditionally manufactured metallic components, fatigue failure in parts manufactured by laser powder bed fusion (LPBF) occurs, mainly due to inherent defects such as residual stresses, internal flaws and surface roughness. An insight into the fatigue behaviour of the LPBF Ti6Al4V alloy is presented here.

Keywords: Fatigue behaviour; LPBF Ti6Al4V; Additive manufacturing; Fatigue life; Fracture surface.

1. Introduction

Additive manufacturing allows the direct creation of near-net shape structures from CAD models by a directed source of heat to fabricate parts, one layer upon another [1]. Such directed sources on energy are either an electron beam or laser beam, that are used to produce metallic parts from powders that are melted in a layer-by-layer manner [2]. Additive manufacturing technologies include, (1) binder jetting, where liquid is deposited as droplets-like shape to bind

powder material; (2) directed energy deposition (DED), which focuses heat energy to melt and bind materials that are provided in a wire or powder form, the former where metallic powder is blasted for combined energy and deposition into a laser beam [3], [4]; (3) material extrusion, is an AM technique where the feedstock is pushed through a nozzle to determine the voxel size [3], a 3D fused deposition modeling (FDM) is commonly used method [5]; (4) material jetting, in which material's droplets are deposited onto a build platform; (5) sheet lamination, here the feedstock is in a shape like a sheet that constitute a layer in the build; (6) Vat polymerization is the process of creating a solid by photolithographically cross-linking of thermoset liquid polymer resins to create a solid; and (7) Powder bed fusion (PBF), where the surface of a powder bed is exposed to a thermal source to that causes fusion of powder[3]. The PBF variants include the major technologies for fabricating metallic parts additively of laser engineered net shaping (LENS), electron beam melting (EBM), selective laser sintering (SLS), as well as direct metal laser sintering (DMLS), or selective laser melting (SLMand[2], [6].

Alloys of titanium are used in automobiles, aerospace, biomedical, energy and marine, and industries, because they possess high strength, high fracture toughness, low density, good resistance against corrosion, and good biocompatibility [2], [7], [8]. The dual phase (α+β) Ti6Al4V alloy is comprised of 6 wt.% α-stabilizing aluminum and 4 wt.% β-stabilizing vanadium, contributing. It is the most widely used alloy of titanium. In the 1950s, the alloy was originally formed for its uses for aircraft components. In addition to its high strength, the alloy is lightweight, and is thus good for the manufacture of gas turbines, jet engines, and some airframe structures [8]. The Ti6Al4V alloy is applied in medium-temperature environments in the range of 250-400 °C [9]. The use of temperatures above 400 °C affects its microstructure and mechanical performance [9] and is thus undesirable. The β-transus temperature, above which only β-phase exists for this alloy, is around 995 °C [10].

According to ASTM International standards, fatigue is localised and permanent damage that occurs progressively in materials exposed to varying stresses and strains, of which after sufficient number of fluctuations leads to the formation of cracks or fracture [11], [12]. Fatigue is characterized by the three consecutive stages of the initiation of cracks, growth of cracks, and fast fracture. Once cracks are initiated, they will continue to grow until they reach a critical length [12], [13]. The continued growth of cracks slowly subtracts area from the cross-section of a loaded component. Components will split into two or more pieces due to rapid crack growth that occurs when the cross-section that is intact is not able to carry the load imposed on it [11], [13]. Fatigue loading may be applied in the various regimes of tension-tension, tension-compression, compression-compression, and reversed bending as well as rotary fatigue loading. Generally, the conclusion made is that tension-compression fatigue is the most severe of these types of loading due to the Bauschinger effect that leads to a gradual reduction in the yield strength of a material with each half cycle [14], [15], [16], [17]. Many factors influence the fatigue behaviour of metals, while components are in service such as mean stress, stress ratio, load regime, type of fluctuating loading, stress concentration, loading frequency, temperature, heat treatment, microstructure, and surface defects [13], [15], [18], [19]. In this paper, the fatigue behaviour of Ti6Al4V produced by the LPBF is reviewed and the various effects that influence fatigue, such as the ones mentioned here, in addition to residual stress, porosity, and the build direction discussed. This is done in order to increase the understanding and the concepts of the fatigue failure, as well as benefits and limitations on the use of the Ti6Al4V.

2. Fatigue Fracture

A fracture can be defined as the division of one solid part into pieces due to an imposed stress. Three stages are considered to comprise the fatigue fracture process: initiation of cracks, growth of cracks, and eventual fracture. Normally cracks initiate at points of stress concentration such

as notches, sharp corners, or inclusions [18]. A typical micrograph showing a fatigue fracture surface and its different zones is shown in Fig. 1.

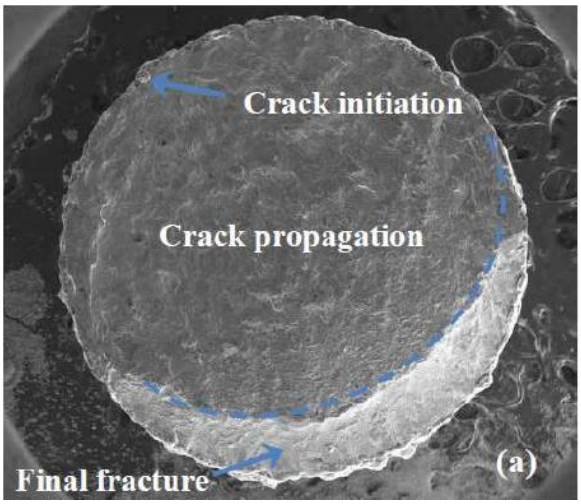

Fig. 1: Fatigue crack initiation and propagation [20]

Crack initiation is a process where cracks are formed in a material. This initial formation of cracks normally occurs because of the pile-up dislocations or from existing imperfections such as surface scratches and internal voids [11]. Initiation of fatigue cracks is dependent on microstructural features and micro-geometry of materials, as well as the nature of the load that is applied. Initiation of cracks are locations of maximum equivalent stress on contact surfaces, for the case of contact mechanical elements [21]. During fatigue testing, most of the number of cycles is consumed while initiating a crack which is estimated to be 90% of the life of a component [12], [22].

Once the crack has been initiated, it grows along high-shear stress planes, in what is referred to as the first stage of fatigue crack propagation. The crack continues to grow until it is slowed by a microstructural obstacle, like inclusions or a grain boundary, that hinders the original direction of the crack growth. The refinement of grains can improve the material's fatigue strength due to the creation of many barriers to the propagation of cracks [23]. The second stage of crack propagation occurs when the applied load is high enough and the crack growth continues with due to the attendant increase of the stress intensity factor, then, in the vicinity of the crack tip, slips begin to form in various planes. In this stage, striations are observable on the fracture surface with the aid of a scanning electron microscope (SEM). On a fracture surface of pure metals and many ductile alloys, fatigue striations can be seen in but not in all engineering materials [23]. Unstable crack growth is the last stage of crack propagation. This process will occur when the magnitude of the stress intensity factor at the tip of the crack equals or exceeds the material fracture's toughness at the specified temperature, loading rate, and environmental conditions [22].

Final fracture occurs when the failure crack is fully grown and the section that is remaining cannot carry the applied load any longer, thus leading to the division of the components into two or more pieces [11].

3. Fatigue S-N curves

Fatigue S-N curves that also go by the name Wohler's curves, such as the one shown in Fig. 2 are used to explain the fatigue life of materials [2]. Stress-based approach has been the standard method of fatigue analysis and design since the mid-19th century. This approach is also known as the S-N approach or stress life [13]. It is the basic method of presenting engineering fatigue

data, which represents the life of the test sample, in several cycles to failure, N, against the stress applied [24]. In this method, fatigue data is presented in the form of semi-log S-N curves. The term semi-log refers to the load cycles, N, plotted as the logarithm to base 10, while the values of stress are plotted as they are [25]. The plots on an S-N curve indicate that the magnitude of stress and number of cycles to fatigue failure are related inversely to one another. In other words, as the stress increases, the material endures a reduced number of cycles to failure [24].

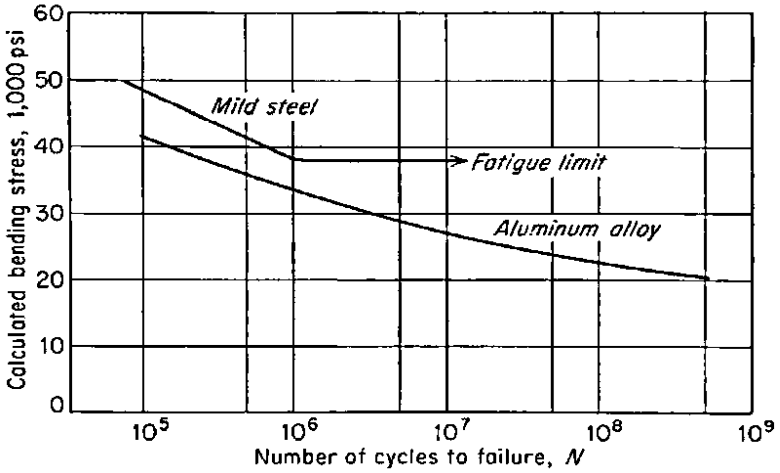

Fig. 2: Typical fatigue S-N curves for ferrous and non-ferrous metal [18]

The total number of fatigue cycles is comprised of the sum of cycles required to initiate a crack and to propagate the crack till complete fracture. Fatigue tests are normally carried out for nonferrous metals at fatigue lives of 10^5, 10^7, and 10^8 cycles for medical, automotive, and aircraft industries, respectively. Metals that undergo strain aging such as steel and titanium have an S-N curve with a sharp knee, whose horizontal part defines the fatigue limit or in other words the endurance limit. A test specimen can endure a limitless number of cycles without failing below this limiting stress line. Almost all nonferrous materials, such as aluminium, copper, and magnesium alloys, have S-N curves that slowly slope downward with an increasing number of cycles. Since the S-N curves of these materials never become horizontal, they lack a true fatigue limit [18].

Mild steel was subjected to fatigue testing, and the results revealed that the resulting S-N curve flattened out and a knee happened at a higher number of cycles, when the content of carbon or nitrogen was lower [18]. Eight to twelve specimens are normally used to determine an S-N curve. Here the first specimen is normally subjected to the highest maximum test stress, where failure is expected after a certain number of cycles. Each subsequent specimen's test stress is reduced until one or more specimens do not fail after a predetermined number of cycles, which is usually at least 10^5, 10^7, and 10^8 cycles for medical, automotive, and aircraft industries, respectively. Fatigue limit is set as the highest stress which was applied at which failure did not occur [18]. During fatigue testing, if a material does not fail before the set number of limiting cycles, that material is deemed to have an infinite life [18]. However, this infinite life does not truly exist for metals that do not depict an S-N curve with a knee, as they will reach their fatigue limit when sufficient fatigue cycles are imposed on them. For some studies, tests are usually cancelled for practical considerations where the design life of components is set for specific applications [11], [18].

4. Factors that Influence the Fatigue Life of Ti6Al4V Alloy

As noted earlier, the fatigue life of Ti6Al4V is affected by several factors including mean stress, stress concentration, stress ratio, load regime, type of fluctuating loading, presence of internal and surface flaws, frequency of loading, temperature, and microstructure, and for additively manufactured parts, the build orientation [13], [15], [18], [26].

4.1. Mean stress

The mean stress (σ_m) is defined by the expression, $\sigma_m = (\sigma_{max} + \sigma_{min})/2$. Fatigue testing is usually performed using fully reversed loading, the term fully reversed indicating that the applied load alternates about zero-mean stress. Most of the time engineering materials are subjected to cyclic loads with a none zero mean stress [13]. The fatigue behaviour is considerably affected by the mean stress. In load control testing, high or intermediate stresses, together with tensile mean stresses lead to significant cyclic creep that increases with increasing mean strain. This cyclical creep exacerbates to the detrimental effects of fatigue through the creation of additional undesirable deformation. In general, a raise in mean stress often causes a decrease in fatigue life [11]. In their work on the influence of mean stress on the fatigue life of LPBF Ti6Al4V, Benedetti et al. [27] and Wycisk et al. [28], confirmed this to be so. Cutolo et al. [29], investigated the manner in which the fatigue strength of the LPBF Ti6Al4V was affected by mean stress and reported that high sensitivity of the specimens to the mean stress. The fatigue strength was observed to reduce in this work, with increasing mean stress [29].

4.2. Stress concentration

Geometric discontinuities such as holes, notches, or fillets, are stress raisers and are inevitable in manufactured parts. Stress raisers reduce fatigue strength [30]. Usually, fatigue cracks in structures, start at such geometrical irregularities. The stress concentration factor (K_t) is defined by the equation, $k_t = \sigma_{max}/\sigma_{nom}$. Surface roughness and metallurgical stress raisers like porosity and inclusions, as well as localised overheating during grinding and decarburization, may as well result in stress concentration. Reducing avoidable stress raisers through careful design and preventing unintentional stress raisers through careful machining and fabrication are by far the best ways to minimise fatigue failure. Specimens with notches on their surfaces generate triaxial states of stress around the notches and stress gradients descending from the roots of the notches towards the centres of the specimens [18].

Baragetti [31], scrutinised the effect notches had on the fatigue behaviour of Ti6Al4V in a study comparing notched and unnotched specimens. He reported that the fatigue limit of the notched specimens was affected after 200 000 load cycles [31]. Ziaja and Kawalec [32], stated that stress concentration leads to fast crack initiation, resulting in short fatigue life, and displays a quasi-cleavage facet fracture feature. Wycisk et al. [28], reported that large defects significantly lead to increased stress concentration and reduction in the lifetime to failure of the LPBF Ti6Al4V samples. The work of Wycisk et al. [28], ties in with that of Jiao et al. [33].

4.3. Frequency of loading

Fatigue life is dependent on loading frequency. During fatigue testing, differences in the frequency of the applied load will give rise to different cycles to fatigue failure. Testing at high frequency can affect the mechanical properties of materials and thus improve their performance in fatigue [15], [18] because of the related high strain rate, strain hardening effect. High frequency testing will on the other hand generate cracks faster that causes the fatigue life of test samples to decrease, since during testing, a large number of cycles are obtained in a short period as compared to low frequency testing. For a project where 10^8 cycles are desired and assuming that there are no mechanical problems with the testing equipment, data for a single S-N curve at low test frequencies would take years to obtain. Therefore, a need for testing at high frequencies [15], [18]. Ritchie et al. [34], studied the manner in which frequency affected high cycle fatigue (HCF) Ti6Al4V samples, loaded in compact-tension at 50 and 200 Hz. When

comparing the results, they observed faster crack growth rate on samples loaded at 50 Hz [34]. This implies that the effect of higher strain rates and related strain hardening was higher than the effect of faster crack growth due to higher load cycles within a given time for the higher cycling frequency. Janeček et al. [35], investigated the behaviour of Ti6Al4V under HCF, at a frequency of 30 and 20 000 Hz. For both frequencies, they observed cleavage facets, and similar fatigue crack initiation sites and crack growth mechanisms, implying that the level of cyclic straining had no effect on the last two characteristics [35].

4.4. Temperature

Temperature does affect the fatigue behaviour of metals and metal alloys. Metals lose fatigue strength as temperatures rise above room temperature [18], [36]. At temperatures greater than half of their melting temperature, creep becomes predominant over fatigue, and the mode of failure changes from inter-crystalline fatigue failure to trans-crystalline creep failure. The amount of creep in metallics will increase with increasing mean stress, at any given temperature [18], [36]. The fatigue life of metals for low-temperature fatigue testing typically increases as temperatures decreases. Walters et al. [37], reported that low temperatures cause a decrease in fatigue crack growth rates. There is no scientific proof that suggests that temperatures lower than the ductile-to-brittle transition temperature cause an abrupt change in fatigue properties, although notch sensitivity in steels increases at low temperatures [18]. The endurance limit of ferrous alloys, which is typically present at room temperature, do not appear when the temperature rises above about 425 °C [19]. An alloy's high-temperature fatigue strength is generally correlated with its creep strength [18], [36].

The S-N curves of Ti6Al4V samples tested at room temperature and at temperatures of 600 K and 700 K are presented in Fig. 3.

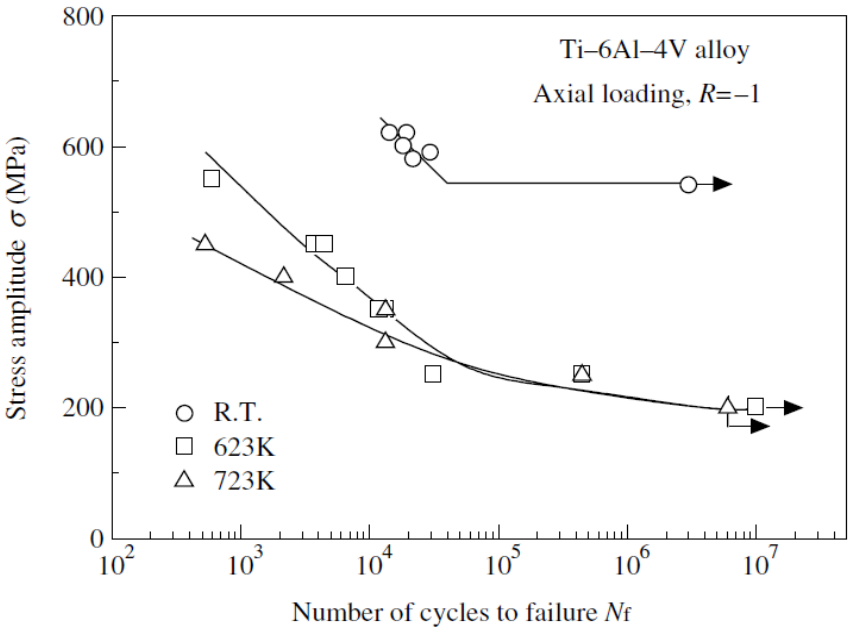

Fig. 3: S-N curves for a Ti6Al4V alloy [38]

Tokaji [38], investigated the influence of elevated temperatures on the behaviour of Ti6Al4V under fatigue loading. At ambient temperature, an endurance limit of 540 MPa was identified at low number of cycles. The author reported that the alloy's fatigue strength is dramatically reduced at elevated temperature as compared to the value at ambient temperature. The author reported that the fatigue strength of the two elevated temperatures showed similar results above 30,000 cycles [38]. Tokaji compared the fracture surfaces of samples of Ti6Al4V that were tested at room temperature on the one hand and at elevated temperatures on the other and

observed ductile fracture at room temperature, and transgranular fracture at elevated temperatures. The author found that at the elevated temperatures of 623 K and 723 K small cracks grew faster than at room temperature. Jiao et al. [39], compared the fatigue crack resistance of SLM Ti6Al4V tested at room temperature and at 400 °C, and found that the fatigue crack growth rate was higher at the latter than at the former test temperatures [39].

Zhu et al. [36], investigated the fracture surface of Ti6Al4V alloy, at room temperature and at a 250 °C. They reported fracture surfaces exhibiting cleavage features at the lower temperature and quasi-cleavage fracture at 250 °C. They further reported the presence of fatigue striations and ductile at both temperatures, which was noted to be a sign of load-interaction effect. They noted that the variation of load within the real random spectrum load history was the source of this load-interaction effect [36]. Pantazopoulos [40] stated that this load-interaction effect and the formation of a compressive stress field prior to the crack tip can decrease the rate of crack propagation. Zhu et al. [36], reported that plastic fatigue striations appeared on both the low and high temperature fracture surfaces, which they concluded was a sign of localized plastic deformation at the crack tip at both temperatures, reflecting significant movement of the crack at each cycle of loading. They further reported that the higher temperature had insignificant influence on the growth rate behaviour of cracks [36]. Arakere et al. [41], the manner in which the fatigue behaviour of Ti-6Al-4V was affected by temperature, at room temperature and at 175 °C, 230 °C, 290 °C, and 345 °C. They reported insignificant changes in growth rates of cracks with changing of test temperatures [41]. It has been reported that the Ti6Al4V alloy is stable at temperatures below 400 °C [9]. This ties in with the report by Zhao et al. [9], that the alloy is suited for application below 400 °C.

From the above-mentioned studies, it can be stated that the fatigue behaviour of Ti6Al4V is affected in a number of ways by temperature. Thus, the fatigue strength of the Ti6Al4V decreases as the test temperature increases, whilst the mode of failure changes from ductile to transgranular fracture, and above a temperature of 345 °C, the rate of propagation cracks increases. Moreover, the mixed ductile quasi-cleavage fracture and brittle cleavage prevalent at room temperature changed to cleavage fracture at 345 °C. Work carried out by the authors elsewhere [42], [43] has demonstrated that the widths of both α-laths and β-laths increased with increasing temperature and with this a decrease and increase of some quasi-static tensile mechanical properties of the alloy.

4.5. Heat treatment

Heat treatment is referred to as a process of heating and cooling metallics that causes the transformation of phases and their microstructures and therefore, changes in their properties [44]. Heat treatment temperature, holding duration, and methods of cooling are parameters that play a vital role heat treatment [45]. Heat treatment is primarily used to regulate microstructure, as well as mechanical properties, particularly strength, hardness, ductility, toughness, and internal stresses [44]. Heat treatment is applied to obtain desired microstructures to increase the strength of a material, remove residual stresses, reduce hardness, and increase ductility [46], [47].

Any operation whether, machining, grinding, welding, or hardening, that involves temperature changes may introduce residual stresses on the surface of a part [22]. By careful selection of temperature and duration, additively manufactured titanium alloys can be stress-relieved with no effect on their ductility or strength [48]. Normally, stress-relieving heat treatment is employed to remove residual stresses that appear because of welding or machining. This preserves shape stability and gets rid of undesirable condition like the loss of yield strength [49], [50], [51]. Increased ductility, fracture toughness, and creep resistance at room temperature, dimensional and thermal stability are the main benefits of annealing titanium and titanium alloys [50]. Solution heat treatment is a heat treatment process where the temperature of an alloy is raised to its beta-phase region and quenched to cause precipitation hardening [22],

[44]. Quenching is a process of rapid cooling of a specimen to acquire specific material properties. This process is normally used to harden and strengthen workpieces and results in a reduction in their fatigue life. Chandramohan et al. [52], reported that β annealing heat treatment for Ti6Al4V can increase ductility by higher than 10% for medical applications. Post-heat treatment, Hot isostatic pressing (HIP). is a procedure in which materials are compressed materials at high temperature and isostatic pressure of up to 2,000 °C and 200 MPa, respectively, at the same time. Argon gas is the most used pressure medium in this process [53]. This technique is employed to reduce porosity, as well as microstructural inhomogeneities that affect the performance of materials in fatigue loading [53], [54].

Frkan et al. [55], studied the manner in which the fatigue life of SLM Ti6Al4V specimens was affected by heat treatment. They observed longer fatigue life for samples that was soaked for four hours at 900 °C than for samples that were soaked for four hours at 740 °C [55]. This is because the samples that are soaked at 900 °C have coarser microstructure that leads to higher ductility and lower tensile strength in them compared to samples that are soaked at 740 °C. Malefane et al. [56], reported that Ti6Al4V(ELI) samples that were first heated to relieve stress and thereafter exposed to high temperature annealing had slightly higher fatigue strength at about 10,000 load cycles than as-built specimens. They further reported that the fatigue cracks initiated from micro-pores near the surface and surface roughness in the as-built and annealed DMLS Ti6Al4V(ELI) parts used in the reported work [56]. Chadstad et al. [57], studied the fatigue life of SLM Ti6Al4V, for as-built, stress-relieved, and HIPed samples. They reported that as-built samples had the lowest fatigue life while the samples that were exposed to HIP exhibited the longest fatigue life. They demonstrated further that the fatigue life of the sample that were exposed to HIP was improved by almost 90% at 10^7 cycles [57]. Leuders et al. [58], investigated the manner in which the HCF behaviour of SLM Ti6Al4V was influenced by heat treatment and HIP. The average fatigue lives recorded in this case were 27,000, 93,000 and 290,000 for as-built, annealed at 800 °C and annealed at 1050 °C, respectively. They reported that for the HIPed samples none of sample failed before 2,000,000 cycles which was taken to be their runout [58]. They demonstrated that even if the size of the pores in the samples was decreased by application of HIP, there were micropores that still remained within the material that would then affect the HCF behaviour of the material [58].

Hasib et al. [59], studied the role of heat treatment processes on the propagation of fatigue cracks in PBF Ti6Al4V samples. The authors found that as-built samples had the lowest near-threshold growth rates fatigue cracks (less than 10^9 m/cycle), followed by HIPed samples at 850 °C and 950 °C, while the highest growth rates of fatigue cracks were exhibited by annealed at 1020 °C[59]. Dhansay [60], studied the effect of heat treatment on the fracture behaviour of LPBF Ti6Al4V under fatigue loading. They observed fracture surfaces dominated by transgranular and faceted quasi-cleavage for stress-relieved, and as-built samples. Dimples were observed for the samples double annealed for two hours at 940 °C, cooled in a furnace to 910 °C and soaked at this temperature for eight hours and then quenched in water, and thereafter aged for two hours at 750 °C and finally, furnace cooled [60]. They further reported that the double annealed samples had more than 50% increase in near threshold stress intensity over the as-built and stress relieved samples [60].

The foregoing studies have shown that as-built Ti6Al4V parts have the lowest fatigue life, and that the fatigue life of Ti6Al4V was significantly improved by post heat treatment. Specimens that were exposed to HIP exhibiting the longest fatigue life except in the study by Hasib et al. [59], where β-annealing led to the longest fatigue life, which is unusual and can be due to a much higher annealing temperature above the β-transus temperature. At high temperatures, thermal energy of atoms increases and causes the atoms to migrate more easily, thus allowing a rearrangement of the microstructure [19] and growth of grains leading to an increase of ductility.

4.6. Microstructure

The microstructure of a material is described by size, shape, and the arrangement of grains. Both the service life and mechanical properties of materials is determined by its microstructure [61]. The crystal structure of titanium alloys that are heat-treated above the β-transus temperature changes from hexagonal closed packed to body centered cubic [42]. The cooling rates imposed thereafter, act as the deciding factors for the parameters of the resulting microstructures [62]. Grain size is also known to affect the fatigue behaviour of Ti6Al4V alloy, such that when the grains become larger fatigue strength decreases while small grains result in higher fatigue strength [63]. At low temperatures the rate of propagation of fatigue cracks decreases, while it increases at high temperatures [37]. However, ductile materials have lower values of stress intensity factor than brittle materials. Therefore, the stress required to cause brittle fracture will be lower than the stress required to cause ductile fracture. Therefore, brittle material will experience faster propagation of cracks than ductile material [64]. Therefore, the growth of fatigue cracks is a complex combination of the different converse trends noted here and in the last paragraph of the previous section. The Ti6Al4V alloy occurs in the various forms shown in Fig. 4.

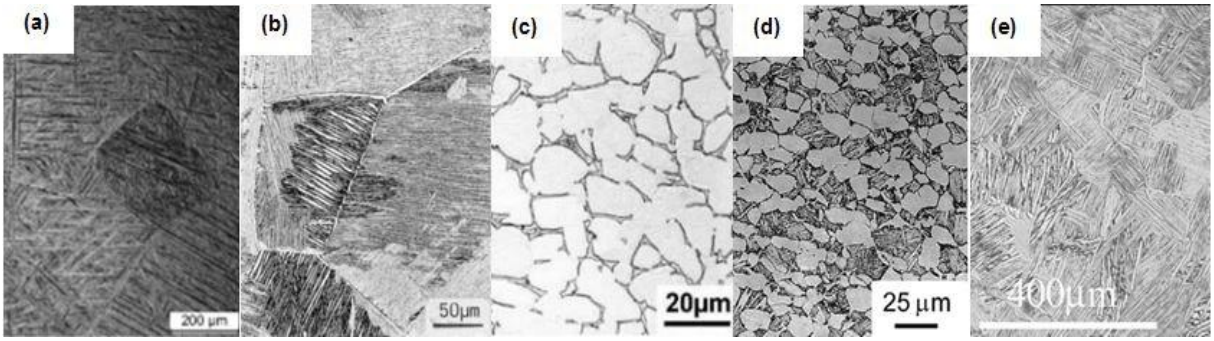

Fig. 4: Microstructures of Ti6Al4V (a) martensitic, (b) lamellar, (c) equiaxed, (d) bimodal, and (e) Widmanstätten [65], [66]

Martensitic microstructure is characterized by the needle-like α'-lath structures shown in Fig. 4(a), is formed through cooling rates higher than 410 °C/s of the alloy from the β-region and has high hardness, strength, and stiffness, and low ductility [67], [68]. The main disadvantage of this microstructure is its high brittleness. The lamellae microstructure shown in Fig. 4(b), consists of alternating layers of α and β and is formed by colling from the β-region.at slow rates. The microstructure is characterized by lower strength and high ductility, as well as better fatigue properties than equiaxed microstructures, with good resistance to the propagation of fatigue cracks. Fig. 4(c) shows the equiaxed microstructure, formed by recrystallization of the alloy from the β-region followed by globulisation that causes the formation of α-grains and β-grains deposited at their grain boundaries. The microstructure has good resistance to the initiation of fatigue cracks but poor resistance to the propagation of fatigue cracks [67], [68]. The bimodal microstructure shown in Fig. 4(d), is formed from recrystallization in the α+β phase-field and consists of primary α-grains and leads to a blend of lamellae and equiaxed microstructures. It has better fatigue properties arising from a combination of good resistance against initiation of fatigue cracks of the equiaxed microstructure, and good resistance to the propagation of fatigue cracks of the lamellae microstructure. The microstructure also has the highest ductility among the five microstructures of Ti6Al4V alloy shown in this figure [4], [69], [70].

The Widmanstätten microstructure shown in Fig. 4(e), is achieved when the alloy is slowly cooled from the β-phase region by air. The hcp α-phase begins to emerge as plates from the β-grain boundaries when the temperature of the alloy drops below β-transus [65]. This microstructure is known to have low strength and low ductility, as well as the poorest fatigue resistance among the different microstructures of Ti6Al4V [71], [72].
Studies have proven that the LPBF Ti6Al4V as-built samples exhibits within the prior β-grains, acicular α' martensite [73], [74], [75]. Lekoadi et al. [45], observed large epitaxial β-grains, with their longer axis being parallel to the build direction of SLM Ti6Al4V as-built samples. These grains grow epitaxially perpendicular to the travel-direction of the laser beam and parallel to the direction of the build. This primarily results from the molten pool's temperature gradient during LPBF processing being nearly perpendicular to the scanning direction [45]. Cao et al. [76], stated that for cracks that are perpendicular to the build direction, the prior β-grains deflect cracks. This means that the boundaries of the epitaxial β-grain boundaries interrupt the cracks resulting in their slow rate of propagation. However, for the cracks that propagate in a direction that is parallel to that of the build, the authors observed that they propagate without much resistance, along the boundaries of the prior β-grains . They demonstrated that the faster growth of cracks occurred along the build direction and would lead to a decrease in fracture toughness because of easier propagation of cracks along the weaker prior β-grain boundaries [76]. This is ties in with the work of Malefane et al. [56]. Cerri et al. [77], saw few microstructural changes when heat-treating as-built parts at 740 °C (which is below the β-transus) for 130 minutes, and noted that the α′ martensite did not completely transform to α+β grains, and that, the prior β-grains remained visible [77]. Neikter et al. [78], observed that the α-grain boundary was dependent on the rate of cooling, where a high rate of cooling rendered thin and α-grain boundaries that were discontinuous, whilst a slow rate of cooling led to thick and continuous α-grain boundaries [78]. Jaber et al. [79], observed differences arising from furnace and water cooling and stated that the size of the α-grains had increased after furnace cooling compared to water cooling. This is because water cooling is rapid and gives rise to fine α-grains, whilst furnace cooling is slow and provides opportunity for the formation of β-grains.
Hasib et al. [59], looked into the role of microstructures on the fatigue response of LPBF Ti6Al4V alloy. They discovered the main factor contributing to resistance of the propagation rate of fatigue cracks was the knees of the α'/α laths. For rates of growth rates that are less than 10^7 cycles, they reported that larger thickness of the α-laths gave rise to a better resistance of the growth of fatigue cracks and higher fatigue thresholds. They demonstrated that above 10^7 cycles, resistance to the growth of fatigue cracks was insensitive to the thickness of the α-laths for samples that were heat-treated [59]. Kunz et al. [80], found the α′ martensitic microstructure to have the smallest resistivity to the growth of fatigue cracks for the as-built DMLS Ti6Al4V alloy [80]. Agius et al. [73], stated that the α′ martensitic grains were significant during the crack initiation stage because they had few long slip bands and therefore, less irreversible slip, which led to the presence of less crack initiation sites [73]. Hosseini [30], stated that the development of equiaxed or lamellar microstructure will lead to shorter fatigue life while the formation of bimodal microstructure is desirable as it resists fatigue crack initiation and propagation [30]. Yuri et al. [81], investigaged the effect of microstructure on the HCF properties of Ti6Al4V, for samples that were furnace cooled, air cooled, and water quenched, separately. They found the width of α-lamellar to be 4 to 12 μm for furnace cooled samples, 2 to 3 μm for air cooled samples and finer α-lamellar for water quenched samples. They reported that, at 10^7 cycles the fatigue strength increased from samples that were quenched in water, cooled in air and cooled in a furnace, in this order [81]. On the other hand, Ziaja and Kawalec [32], annealed Ti6Al4V samples at 850 °C and 910 °C and observed average grain diameters of 8.8 μm and 8.2 μm, respectively. They reported that lower volume fractions of the α-laths led to a longer fatigue life [32]. This was probably a result of the α-phase being stronger that

the β-phase and its reduction in volume fraction will, therefore, lead to an increase of ductility and attendant increase of fatigue life.

4.7. Surface roughness

Approximately 90% of all in-service fatigue failure starts at the surfaces of components [18]. It is known that in bending and torsional loading, that the maximum stress occurs at the surface, and failure is thus expected to start there [18]. Chern et al. [82], observed that the fatigue strength of AM parts was most affected by surface roughness as . Normally, the fatigue life increases with decreasing roughness of surfaces and vice vasa, as better roughness surfaces minimises local stress raisers [18]. As a result, the surface preparation of fatigue test specimens needs particular attention. It is essential to have a surface finish free of grinding scratches and machining grooves [12]. Carrion et al. [83], in their study of fully reversed loading of Ti6Al4V ELI samples with a fully equiaxed microstructure, reported that cracks were initiated at sites of inclusions near surfaces. They observed shorter fatigue life for specimens with large sizes of inclusions [83]. Vayssette et al. [84], carried out a HCF test on SLM Ti6Al4V samples and observed an increase in fatigue strength from as-built samples to machined samples. Edwards and Ramulu [26] and Wycisk et al. [85], observed longer fatigue life on machined SLM Ti6Al4V specimens compared to as-build specimens. It was observed that machining samples removed roughness on their surfaces, thus reducing stress concentration effects, with resulting longer fatigue lives of parts that were manufactured additively [86]. Wycisk et al. [87], investigated the high cycle fatigue performance of SLM Ti6Al4V as-built and polished, as well as shot-peened samples. They observed a much lower fatigue limit of 210 MPa for as-built samples compared on of 510 MPa upon polishing. For the shot-peened samples they recorded a 15% reduction of the fatigue limit as compared with the polished samples. This was an unexpected trend, suggesting that crack initiation was due to internal pores [87].

4.8. Residual stresses and porosity in LPBF

In LPBF, the energy of the laser beam is configured to liquefy the layer of metallic powder entirely by heat from the point of application and across its entire thickness. To ensure that every run s overlaps slightly, the previous pass and goes through the layer of powder at the top, the scanning speed, hatch distance, and laser beam power are adjusted. As a result, homogenous solids are produced by ensuring that strong metallic bonds form between adjoining tracks and layers. The build table descends one layer thickness after a layer has been printed, and a fresh layer of powder depositing on the build platform before being levelled with a re-coater blade and printing commenced once more. Until the part is finished, this cycle continues. The building platform delivers heat as well so that the molten part solidifies swiftly. In order to protect parts from oxidation, the chamber is usually pumped with a gas environment. The width of the one layer of powder is typically 0.020 to 0.100 mm. The as-built parts may exhibit some structural defects because of the unbalanced stress profile in between the layers of the build part during processing [88]. The EBM build parts are liable to less residual stresses than the LPBF parts since the build environment is a maintained at temperatures, ranging from 600-700 °C. Titanium alloy parts that are exposed to this temperature for longer periods during fabrication, will have lower values of residual stresses [6].

Residual stresses can be defined as self-equilibrium stresses of deformed material that persist inside a structure after removal of the loads causing the deformation. Residual stresses in additive manufacturing are formed when solidified printed layers inhibit contraction of the newly fused layer. They can result in initiation of cracks, and delamination, and can decrease the fatigue life of a part [88]. Using optimum process parameters or post-heat treatment processes can reduce residual stresses [6]. Stress relieving is employed to decrease or remove unwanted residual stresses occurring in built metallic components. and is carried out with no influence on the their mechanical properties. This procedure ensures that the shapes of built parts remain stable [49], [50], [51]. Other mechanical treatment like surface rolling or shot-peening are applied to reduce residual stress [6]. Common defects in additive manufacturing

include pores formed by entrapped gases and lack-of-fusion[82]. The formation of these gas pores is a result of trapped gas when the metal is still molten as it solidifies quickly [89]. It was observed that samples that fail due to this type of defect have longer fatigue life as compared to the case of other AM defects [57]. Lack-of-fusion pores, which are usually found in between layers, grow in a direction that is orthogonal to the direction of build [82]. They are developed because of powder that is not fully melted [89]. They can affect the fatigue life of metals than gas pores [90]. Porosity contributes to shorter fatigue life in LPBF samples, especially for the case of internal defects that are located near the surface. A micro-CT scanner is usually used to examine porosity. Due to variations of contrast between scans, the type of metal and pore-sizes in relation to the resolution of scanning, as well as due to limited time for the analysis of scans, some pores can be missed [90]. The issue of porosity and defects in the microstructure can affect the tensile properties of built parts and is solved by optimizing the DMLS parameters [91]. To have the best mechanical properties, maximum density should be achieved. To build non-porous DMLS parts, the process parameters of layer thickness, scanning speed, laser powder, , and other process parameters must be optimum [92]. The influence of porosity and residual stress on the fatigue behaviour of materials is not as severe as that of the microstructure [57]. Fig. 5 shows various forms of defects on fatigue failure surfaces of the LPBF Ti6Al4V alloy.

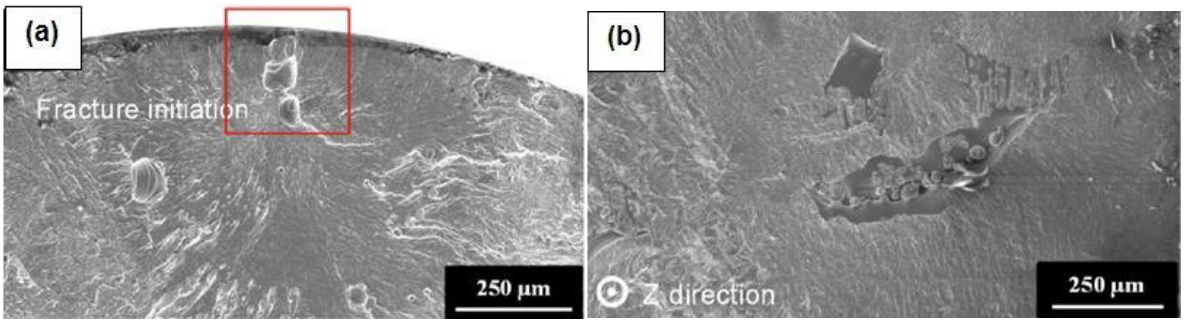

Fig. 5: Micrographs showing types of defects (a) porosities and (b) unmelted zones on Ti6Al4V parts [57]

Benedetti et al. [27], studied fatigue behaviour of SLM Ti6Al4V(ELI) specimens and found that crack initiation sites were due to larger internal defects located near the surfaces. Fotovvati et al. [86], claimed that the effect of internal pores on fatigue behaviour were less significant compared to surface defects. Edwards and Ramulu [26], reported that both porosity and residual stresses, caused the fatigue strength of SLM Ti6Al4V to be lower than that of wrought Ti6Al4V parts [26]. Gong et al. [20], found defects to be very detrimental on the performance of SLM Ti6Al4V fatigue specimens, as cracks initiate there. Le V. D. et al. [93], reported that for the machined Ti6Al4V specimens, cracks initiated at sites of lack of fusion and gas pores, both near the surfaces and within the samples. For as-built samples, cracks were initiated because of lack of fusion on the surfaces and due to the roughness of the surface. They demonstrated that lack of fusion pores will likely cause initiation of cracks in additively manufactured samples [93]. Wycisk et al. [87], investigated the cause of failure in as-built and polished samples of SLM Ti6Al4V. They reported that for the polished samples, cracks that resulted in fracture initiated due to internal pores, while for the as-built samples, cracks initiated due to rough surfaces. It was also reported that as-built samples exhibited shorter fatigue life, while polished samples had longer fatigue life [87]. Methods like the Archimedes principle, X-ray computed tomography, gas pycnometry are first applied to detect defects [86]. Thereafter, the HIP process can be used to lower the degree defects like lack-of-fusion and gas pores of AM parts to improve their fatigue life. However, if these pores are formed at the surface, in which case they are referred to as open pores, they pose a problem of their removal using post-processing operations [53]. The only available method to reduce these pores is to make sure that the optimum process parameters are used in printing [92].

4.9. Process parameters of the LPBF

Additively manufactured parts are produced with set process parameters. The critical ones and ones that can be varied easily by AM machine operators include hatch distance, laser power, laser diameter, scanning speed, , , and layer thickness [86]. Moletsane [92], stated that to produce non-porous DMLS parts, the process parameters like scanning speed, layer thickness, and laser power must be optimal. Wang et al. [94], reported that lower values of laser power will likely produce parts with lack of fusion powder, while high values of laser power will reduce the fluidity (recognized here as a result of reduced viscosity and surface tension) of the melt pool and therefore, causing spattering. They stated that lower scanning speeds can lead to the injection of large amounts of laser energy into the particles of powder and therefore, formation of unstable molten pool flow, while high scanning speeds result in poor overlap of tracks and large interlayer-gaps [94], due to the formation of tracks with irregular cross-sections. The powder material will not melt completely due to limited dwell time, if the laser scanning speed is too high. Too low values of scanning speed lead to overexposure of powder to the laser beam and thus, the creation of voids and formation of wider and shallower tracks [94]. Fotovvati et al. [86], reported that raising of scanning speed will increase porosity because of not enough time for melting of the powder. They also demonstrated that low scanning speed or high laser power are detrimental because they cause the production of parts with porosity [86]. Clearly, optimal process parameters are essential. It was reported that by optimizing process parameters, residual stresses are lowered [73]. Several studies [73], [74], [75], have proven that utilizing a scanning strategy that makes use of the heating of new layers by the residual heat in previous layers and a very tight hatch distance in as-built SLM Ti6Al4V contains the formation of martensitic α' microstructure and will lead to the development of a microstructure with α' and (α + β) grains [73].

4.10. Build-direction

The AM build platform is set with the cartesian coordinates directions shown in Fig. 6, as reference axes,. The lengths of built parts are normally placed orthogonal and parallel to the direction of motion of re-coaters, which is either the x- or y-direction. The z-direction is the normal direction of build as the but both the x- and y-axis directions can also serve as built directions [95].

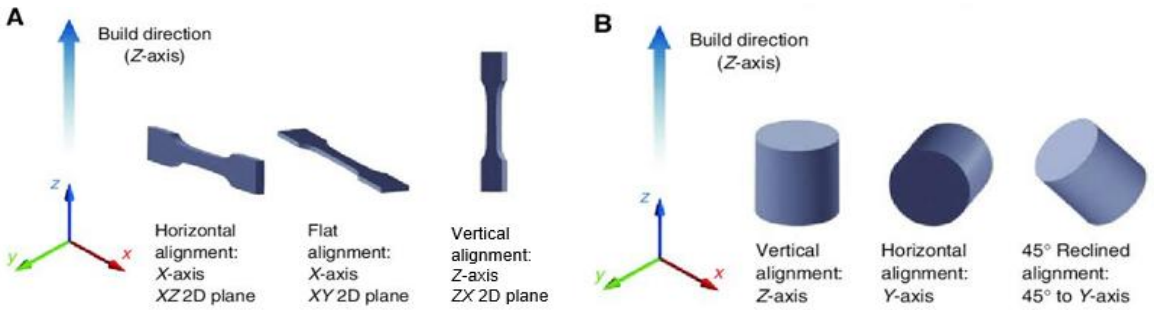

Fig. 6: Build directions in AM [96]

The direction in which structures are built influences the material's mechanical properties. Several studies have revealed that parts build horizontally often resulted in a higher mechanical performance compared to those built vertically [52], [82], [97]. Chandramohan et al. [52], observed fine martensite on the metallography of both horizontally and vertically build parts. Knowles et al. [98], stated that residual stresses that remain within the as-built parts will affect the yield strength of built parts in either the horizontal or vertical directions. Due to the different principles of the various AM technologies in existent and due to the direction build directions used, differences in structure, mechanical, or fatigue properties will exist [91]. This is finding similar to the work of the authors [56].

Malefane et al. [56], investigated how the S-N curves for the DMLS Ti6Al4V(ELI) samples annealed at a temperature of 950 °C were affected by the build direction. They reported that the endurance limit and cycles to failure for samples built in the x- and y-directions were 450 MPa for a run-out of 5,000,000 cycles, and for the z-direction 486 MPa for 1,183,000 cycles [56]. Scanning electron fractographs of a specimen that was built in the x-direction and loaded at a maximum stress of 675 MPa, that fractured at 896,033 cycles in their work are shown in Fig. 7 [56].

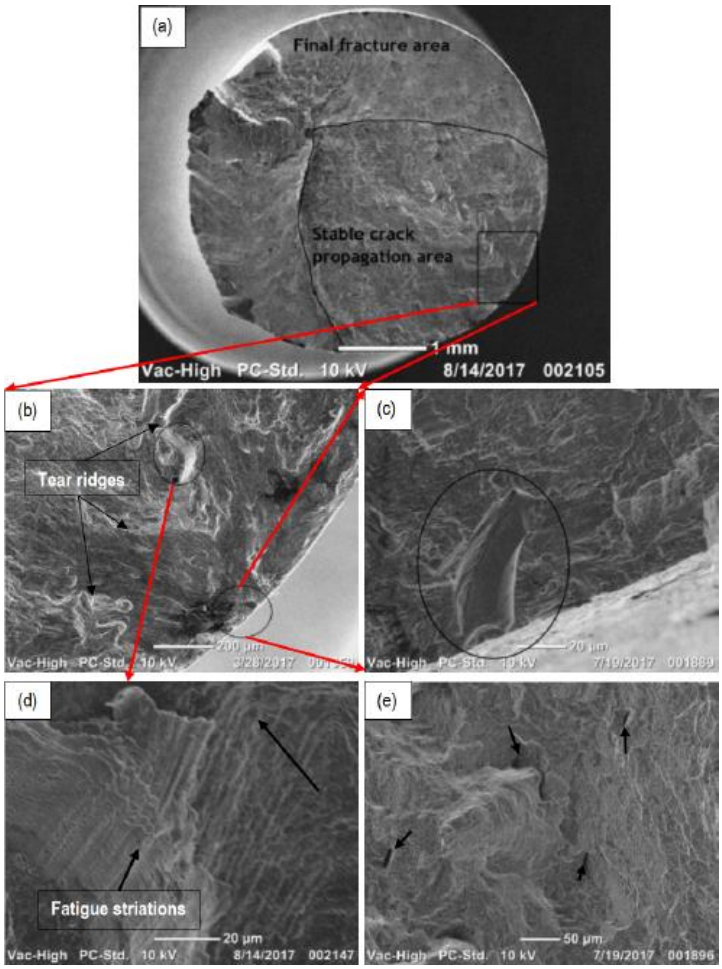

Fig. 7: Fractographs of a DMLS Ti6Al4V (ELI) fractured sample (a) overall fracture, (b) magnification around the crack growth zone, (c) More magnification of 7(c), (d) high magnification and (e) magnification of the shear lip zone [99]

The overall fractograph in Fig. 7(a) shows tear ridges across the whole region of crack propagation, which are characteristics of stable crack growth. Fig. 7(b) shows a magnified portion of Fig. 7(a) with tear ridges and fatigue striations. Fig. 7(c) shows magnified fatigue striations within a circle that are also encircled in Fig. 7(b), which occur on the face of a tear ridge located near an area of crack initiation. The micrograph in Fig. 7(d) illustrates fine striations emanating from a pore that serves as a site for initiation of a crack. The direction of the arrow in this figure points to the alignment of the striations. The fine fatigue striations seen in this figure are indicative of a high number of cycles. Tear ridges are evident in the area of stable crack propagation in Fig. 7(a) and show up in Fig. 7(b) as well. As shown by arrows in Fig. 7(e), internal micropores were observed and it was reported to have elongated in the tear ridges' direction. Malefane [99], reported that for specimens that were built in the z- and y-directions, crack initiation was due to AM surface pores, and shallow dimples were observed, as well as shear regions.

Edwards and Ramulu [26], reported higher fatigue limits for specimens build in the x-direction and lower fatigue limits for specimens whose build was in the z-direction. They assumed that the specimens whose build was in the z-direction, which was also the longitudinal direction of the columnar β-grains, the reason for the lower fatigue limit could be due to long oriented slip planes parallel to the columnar grains. They further reported that specimens whose build was along the z-direction had the roughest fracture surfaces after fatigue testing with loading along this direction [26]. Liu et al. [100], studied fatigue response of SLM Ti6Al4V test pieces built vertically and horizontally. They also reported that cracks initiated because of a lack of fusion for the two build directions. They observed that specimens that were built horizontally, had a higher number of cycles to fatigue failure compared to vertically built specimens [100]. Leuders et al. [58], recorded higher fatigue resistance on SLM Ti6Al4V specimens that were built in the zx-direction than those that were built in the xz-direction [58]. Chan et al. [101], demonstrated that the fatigue strength along both the build directions, x and y was higher compared the one along the z-build direction. They reported that this was because of lack of fusion pores, which were located in between layers that were orthogonal to the loading z-build direction specimens [101]. Dhansay [60], observed larger transgranular cleavage facets in the zx-build direction than in the xz- and xy-build directions for the samples that were double annealed. The author reported that this was likely because of the zx-direction's crack plane and direction of orientation of grains, which favoured faceted fracture more than in the xz- and xy-build directions [60]. Dhansay [60], observed the samples built in the zx-build direction to have the highest residual stresses as compared to the samples built in the xz- and xy- directions. The author further reported that the samples built along the xy-direction depicted the lowest residual stresses [60]. Ter Haar and Becker [102], studied the martensitic microstructure of SLM Ti6Al4V. They reported different aspect ratios of α′ laths in the zx-, xz- and xy-build directions [102]. In contrast Cain et al. [103], investigated the impact build direction has on the propagation of cracks and fracture toughness of SLM Ti6Al4V samples in the xy and xz build directions. They reported that the xy- and xz-build directions had less influence on the rate at which fatigue crack grows and fracture toughness [103]. Hasib et al. [59], found that the near-threshold fatigue crack propagation rate was not significantly affected by the build direction. On other hand, Xu et al. [104], reported that samples built at 0° and 45° had greater fracture toughness than the samples built at 90°.

5. Conclusions

This review paper attempts to provide insight on the influence of mean stress, stress concentration, loading frequency, temperature, heat treatment, microstructure, surface roughness, residual stress and porosity as well as the build direction of the LPBF Ti6Al4V alloy. The following can be deduced from the study:

- The fatigue life of Ti6Al4V reduced with increasing mean stress.
- Loading at different frequencies leads to different number of cycles to failure.
- At elevated temperatures cracks grow faster compared to the case at lower temperatures.
- Increasing temperature led to a decrease of the fatigue strength of Ti6Al4V.
- By changing he microstructure of T6Al4V, post heat treatment processes cause changes in the mechanical properties the alloy.
- The α' martensitic microstructure of LPBF as-built parts causes them to exhibit low fatigue lives.
- Thinner α-laths resist growth of fatigue cracks less than thicker α-laths .
- Amongst the microstructures of Ti6Al4V, the bimodal microstructure is the most desirable as it has a combination of good resistance to both the propagation and initiation of fatigue cracks. The microstructure also has the highest ductility of all the microstructures of the alloy.

- The SLM as-built samples with rough surfaces have lower fatigue lives compared to samples that are machined, polished, or shot peened.
- Optimisation of process parameters reduces porosity and this way minimises its negative effects on the fatigue life of Ti6Al4V.
- Hot isostatic pressing is employed to reduce residual stresses and porosity thus causing an improvement of fatigue performance by up to 90%.
- The samples built horizontally have longer fatigue lives compared to the samples built vertically.

Gaps and Recommendations for Future Work

Fatigue testing at temperatures below 350 °C has been reported [41], to have insignificant effect on the fatigue behaviour of Ti6Al4V samples. This can be because the two mechanical properties (ductility and tensile strength) had equal and opposing effects which resulted in negligible effects on the fatigue behaviour. It was reported in refs. [39], [105], [106], that raising temperature caused an increase of ductility and attendant reduction of tensile strength of the alloy. Moreover, it was noted that an increase in the ductility of the alloy caused its fatigue strength to increase, while a reduction of the strength of the alloy reduced its fatigue strength [107]. The relationships between the increase in test temperature and these two mechanical properties are of great importance, and the temperature at which the significance of these two trends change needs to be thoroughly studied. This is particularly important given the results of some studies [38], [39], that higher temperatures lead to a reduction of the fatigue strength Ti6Al4V. It is essential to pinpoint the temperatures at which the fatigue strength starts weakening and to identify the prevailing fatigue trends with further increase of test temperature for different metallics beyond this point.

It was reported [18] that testing at high frequency will lead to faster generation of cracks and the attendant decrease in the fatigue life of test samples. In contrast the fatigue performance of the materials is improved by testing at high frequencies, because of the arising strain hardening effect that is a consequence of the multiplication and entanglement of dislocations in the course of deformation [15], [18]. These two phenomena and their interplay should be investigated further for different metal alloys.

It was reported [56] that the LPBF samples built in the x-direction had similar microstructures as those built in the y-direction. Therefore, the expectation that the samples will have similar fatigue behaviour, as this is dependent on microstructure. However, the fatigue behaviour of these two sets of samples has been reported to have significant differences. The cause of these differences should be investigated further.

Laser-powder-bed-fusion manufactured parts are considered less reliable for certain applications, because of their poor surface finish. Because of this, LPBF parts require some post-processing such as machining to improve their surface finish. Studies reported in references [84], [26], [85], showed that for machined LPBF Ti6Al4V samples, the values of fatigue strength were higher than those of as-built samples that are known to have rough surfaces. Therefore, there is a need to produce LPBF parts with better surface finish to improve their performance under fatigue loading, and ways of improving the LPBF process should be looked into.

Laser-powder-bed-fusion parts have inherent shortcomings such as residual stresses and internal flaws, that have significant effects on the fatigue life of Ti6Al4V, the latter as many studies have reported that fatigue initiates from such defects. It has been demonstrated that these shortcomings can be minimised by use of optimum process parameters the manufacture of LPBF components. The use of HIP is reported to reduce the number and size of these defects and is this way leads to an improvement of fatigue life by up to 90%. Investigations on how to further reduce these internal defects are essential.

It is noted that most studies, as is the case here are conducted at different values of stress ratios. This makes it difficult to compare the results from such different studies as different stress ratios

lead to different maximum stresses and therefore, different extends of plastic deformation. Another issue that makes it difficult to compare the studies is the different geometries of specimens and the different standards used, and a study to harmonise them is necessary.

Declaration of competing interest

The authors declare that they have no known competing financial interests or personal relationships that could have appeared to influence the work reported in this paper.

Data availability

No data was used for the research described in the article.

Acknowledgement

The authors gratefully acknowledge the Collaborative Program in Additive Manufacturing (CPAM) (Contract no CSIR-NLC-CPAM-21-MOA-CUT-03), for their financial support.

References

[1] T. H. Becker, M. Beck, and C. Scheffer, '14 th International RAPDASA conference held at the Central University of Technology in South Africa in 2013', 2013.

[2] A. Sterling, N. Shamsaei, B. Torries, and S. M. Thompson, 'Fatigue Behaviour of Additively Manufactured Ti-6Al-4 v', in Procedia Engineering, Elsevier Ltd, 2015, pp. 576–589. doi: 10.1016/j.proeng.2015.12.632.

[3] D. Bourell et al., 'Materials for additive manufacturing', CIRP Ann Manuf Technol, vol. 66, no. 2, pp. 659–681, 2017, doi: 10.1016/j.cirp.2017.05.009.

[4] R. K. Nalla, B. L. Boyce, J. P. Campbell, J. O. Peters, and R. O. Ritchie, 'Influence of microstructure on high-cycle fatigue of Ti-6Al-4V: Bimodal vs. lamellar structures', in Metallurgical and Materials Transactions A: Physical Metallurgy and Materials Science, Minerals, Metals and Materials Society, 2002, pp. 899–918. doi: 10.1007/s11661-002-0160-z.

[5] A. Dehghanghadikolaei and B. Fotovvati, 'Additive Manufacturing Methods A Brief Overview', 2018. [Online]. Available: https://www.researchgate.net/publication/327701079

[6] N. Shamsaei and J. Simsiriwong, 'Fatigue behaviour of additively-manufactured metallic parts', in Procedia Structural Integrity, Elsevier B.V., 2017, pp. 3–10. doi: 10.1016/j.prostr.2017.11.053.

[7] J. Günther et al., 'Fatigue life of additively manufactured Ti–6Al–4V in the very high cycle fatigue regime', Int J Fatigue, vol. 94, pp. 236–245, Jan. 2017, doi: 10.1016/j.ijfatigue.2016.05.018.

[8] S. Liu and Y. C. Shin, 'Additive manufacturing of Ti6Al4V alloy: A review', Mater Des, vol. 164, p. 107552, Feb. 2019, doi: 10.1016/J.MATDES.2018.107552.

[9] J. R. Zhao, F. Y. Hung, T. S. Lui, and Y. L. Wu, 'The relationship of fracture mechanism between high temperature tensile mechanical properties and particle erosion resistance of selective laser melting Ti-6al-4v alloy', Metals (Basel), vol. 9, no. 5, May 2019, doi: 10.3390/met9050501.

[10] C. C. Murgau, 'Microstructure Model for Ti-6Al-4V used in Simulation of Additive Manufacturing Material Mechanics', Lulea University of Technology, Lulea, 2016.

[11] F.C. Campbell, Elements of Metallurgy and Engineering Alloys. ASM International, 2008.

[12] H. E. Boyer, Atlas of Fatigue Curves. Ohio: ASM lnternatlonal, 1986. [Online]. Available: www.asminternational.org

[13] Y. Lee, J. Pan, R. Hathway, and M. Barkey, Fatigue Testing and Analysis (Theory and Practice). Burlington: Elsevier Butterworth Heinemann, 200, 2005.

[14] A. Mouritz, Introduction to Aerospace Material. Woodhead Pub, 2012.

[15] A. J. Belinky, 'High cycle compressive fatigue of unidirectional glass/polyester performed at high frequency', Montana, 1994.
[16] K. Lietaert, A. Cutolo, D. Boey, and B. Van Hooreweder, 'Fatigue life of additively manufactured Ti6Al4V scaffolds under tension-tension, tension-compression and compression-compression fatigue load', Sci Rep, vol. 8, no. 1, Dec. 2018, doi: 10.1038/s41598-018-23414-2.
[17] D.R. Moss and M. Basic, Pressure vessel design manual, Fourth edition: Chapter 8 on high pressure vessel. 2010.
[18] G.E. Dieter, Metallurgy and Metallurgical Engineering. New York: McGRAW-HILL BOOK COMPANY, 1961.
[19] F.C. Campbell, Fatigue and Fracture. Ohio: ASM International, 2012.
[20] H. Gong, H. K. Rafi, K. Rafi, T. Starr, and B. Stucker, 'Effect of defects on fatigue tests of as-built TI-6AL-4V parts fabricated by selective laser melting', 2012. [Online]. Available: https://www.researchgate.net/publication/279687860
[21] S. Glodez, J. Flasker, and Z. Ren, 'Crack initiation and crack propagation in the contact area of two cylinders', 1996. [Online]. Available: www.witpress.com,
[22] A. Blake, Handbook of Mechanics, Material and Structures. Arizona: A Wiley-Interscience Publication, 1985.
[23] G. Totten, 'Fatigue Crack Propagation', Advanced Materials & Processes, 2008, [Online]. Available: www.asminternational.org
[24] J. William D. Callister and David Rethwisch, Material Science and Engineering - An introduction, 10th ed. John Wiley & Sons, Inc, 2018.
[25] M. Pedersen, 'Introduction to Metal Fatigue-Concepts and Engineering Approaches', 2018, doi: 10.13140/RG.2.2.25216.28163.
[26] P. Edwards and M. Ramulu, 'Fatigue performance evaluation of selective laser melted Ti–6Al–4V', Materials Science and Engineering: A, vol. 598, pp. 327–337, Mar. 2014, doi: 10.1016/J.MSEA.2014.01.041.
[27] M. Benedetti, V. Fontanari, M. Bandini, F. Zanini, and S. Carmignato, 'Low- and high-cycle fatigue resistance of Ti-6Al-4V ELI additively manufactured via selective laser melting: Mean stress and defect sensitivity', Int J Fatigue, vol. 107, pp. 96–109, Feb. 2018, doi: 10.1016/j.ijfatigue.2017.10.021.
[28] E. Wycisk, S. Siddique, D. Herzog, F. Walther, and C. Emmelmann, 'Fatigue performance of laser additive manufactured Ti–6Al–4V in very high cycle fatigue regime up to 109 cycles', Front Mater, vol. 2, Dec. 2015, doi: 10.3389/fmats.2015.00072.
[29] A. Cutolo, C. Elangeswaran, and B. Van Hooreweder, 'On the Effect of the Stress Ratio on Fatigue Properties of Ti-6Al-4V Produced by Laser Powder Bed Fusion', Material Design & Processing Communications, vol. 2022, pp. 1–7, Feb. 2022, doi: 10.1155/2022/3530603.
[30] S. Hosseini, 'Fatigue of Ti-6Al-4V', in Biomedical Engineering - Technical Applications in Medicine, InTech, 2012. doi: 10.5772/45753.
[31] S. Baragetti, 'Notch corrosion fatigue behavior of Ti-6Al-4V', Materials, vol. 7, no. 6, pp. 4349–4366, 2014, doi: 10.3390/ma7064349.
[32] W. Ziaja and A. Kawalec, 'Dwell Fatigue Behavior of Two-Phase Ti-6Al-4V Alloy at Moderate Temperature', JOM, vol. 74, no. 10, pp. 3745–3751, Oct. 2022, doi: 10.1007/s11837-022-05461-3.
[33] Z. Jiao, X. Wu, H. Yu, R. Xu, and L. Wu, 'High cycle fatigue behavior of a selective laser melted Ti6Al4V alloy: Anisotropy, defects effect and life prediction', Int J Fatigue, vol. 167, Feb. 2023, doi: 10.1016/j.ijfatigue.2022.107252.
[34] R.O. Ritchie, D.L. Davidson, B.L. Boyce, J.P. Campbell, and O. Roder, 'High-cycle fatigue of Ti-6Al-4V', Fatigue Fracture Engineering Material Structure, vol. 22, pp. 621–631, 1999.

[35] M. Janeček et al., ‘The very high cycle fatigue behaviour of Ti-6Al-4V alloy’, in Acta Physica Polonica A, Polish Academy of Sciences, Oct. 2015, pp. 497–502. doi: 10.12693/APhysPolA.128.497.
[36] Y. ZHU, J. XIONG, Z. LV, and Y. ZHAO, ‘Testing and evaluation for fatigue crack propagation of Ti-6Al-4V/ELI and 7050-T7452 alloys at high temperatures’, Chinese Journal of Aeronautics, vol. 31, no. 6, pp. 1388–1398, Jun. 2018, doi: 10.1016/j.cja.2017.06.013.
[37] C. L. Walters, ‘The Effect of Low Temperatures on the Fatigue of High-strength Structural Grade Steels’, Procedia Materials Science, vol. 3, pp. 209–214, 2014, doi: 10.1016/j.mspro.2014.06.037.
[38] K. Tokaji, ‘High cycle fatigue behaviour of Ti–6Al–4V alloy at elevated temperatures’, Scr Mater, vol. 54, no. 12, pp. 2143–2148, Jun. 2006, doi: 10.1016/J.SCRIPTAMAT.2006.02.043.
[39] Z. H. Jiao, R. D. Xu, H. C. Yu, and X. R. Wu, ‘Evaluation on Tensile and Fatigue Crack Growth Performances of Ti6Al4V Alloy Produced by Selective Laser Melting’, in Procedia Structural Integrity, Elsevier B.V., 2017, pp. 124–132. doi: 10.1016/j.prostr.2017.11.069.
[40] G. Pantazopoulos, ‘A Short Review on Fracture Mechanisms of Mechanical Components Operated under Industrial Process Conditions: Fractographic Analysis and Selected Prevention Strategies’, Metals (Basel), vol. 9, no. 2, p. 148, Jan. 2019, doi: 10.3390/met9020148.
[41] N. K. Arakere, T. Goswami, J. Krohn, and N. Ramachandran, ‘High Temperature Fatigue Crack Growth Behavior of Ti-6A1-4V’, High Temperature Materials and Processes, vol. 21, no. 4, 2011.
[42] A. Shaikh, S. Kumar, A. Dawari, S. Kirwai, A. Patil, and R. Singh, ‘Effect of temperature and cooling rates on the α+β morphology of Ti-6Al-4V alloy’, in Procedia Structural Integrity, Elsevier B.V., 2019, pp. 782–789. doi: 10.1016/j.prostr.2019.07.056.
[43] D. Zöllner, ‘Impact of a strong temperature gradient on grain growth in films’, Model Simul Mat Sci Eng, vol. 30, no. 2, Mar. 2022, doi: 10.1088/1361-651X/ac44a8.
[44] ASM International, ‘Heat treating’, Ohio, 2015. Accessed: Mar. 15, 2024. [Online]. Available: https://www.amgindustries.com/ASM%20Subject%20Guide_HeatTreating.pdf
[45] P. Lekoadi, M. Tlotleng, N. Maledi, and & B. N. Masina, ‘Effect of heat treatment on microstructure, hardness and tensile properties of high-speed selective laser melted Ti6Al4V’, in 2022 RAPDASA-RobMech-PRASA-CoSAAMI Conference, Pretoria: CSIR, 2022.
[46] Z.B. Fuad, ‘Effect of Heat Treatment on Fatigue Life’, Universiti of Malaysia Pahang, Malaysia, 2012.
[47] R. Fragoudakis, S. Karditsas, G. Savaidis, and N. Michailidis, ‘The effect of heat and surface treatment on the fatigue behaviour of 56SiCr7 spring steel’, in Procedia Engineering, Elsevier Ltd, 2014, pp. 309–312. doi: 10.1016/j.proeng.2014.06.268.
[48] K. P. Anil Rajagopal, A. Mathew Jose, A. Soman, C. J. Dcruz, and N. N. Sankar, ‘INVESTIGATION OF PHYSICAL AND MECHANICAL PROPERTIES OF Ti ALLOY (Ti-6Al-4V) UNDER PRECISELY CONTROLLED HEAT TREATMENT PROCESSES’, 2015. [Online]. Available: www.jifactor.com
[49] Ó. Teixeira, F. J. G. Silva, L. P. Ferreira, and E. Atzeni, ‘A review of heat treatments on improving the quality and residual stresses of the Ti–6Al–4V parts produced by additive manufacturing’, Aug. 01, 2020, MDPI AG. doi: 10.3390/met10081006.
[50] R. R. Boyer, ‘Titanium and Its Alloys: Metallurgy, Heat Treatment and Alloy Characteristics’, in Encyclopedia of Aerospace Engineering, Wiley, 2010. doi: 10.1002/9780470686652.eae198.

[51] Frederick H. Mueller, Heat Treatment and Properties of Iron and Steel. National Bureau of Standards Library, 1960.
[52] P. Chandramohan, S. Bhero, A. Obadele, P. A. Olubambi, and & B. Ravisankar, 'Effect of built orientation on direct metal laser sintering of Ti-6Al-4V', Indian Journal of Engineering & Materials Sciences, vol. 25, pp. 69–77, 2018.
[53] J. Carlos and C. Santos, 'A Qualification Methodology for Additively Manufactured Parts', Repositorio Aberto da Universidade do Porto, Porto, 2016.
[54] D. Greitemeier, F. Palm, F. Syassen, and T. Melz, 'Fatigue performance of additive manufactured TiAl6V4 using electron and laser beam melting', Int J Fatigue, vol. 94, pp. 211–217, Jan. 2017, doi: 10.1016/j.ijfatigue.2016.05.001.
[55] M. Frkan, R. Konecna, G. Nicoletto, and L. Kunz, 'Microstructure and fatigue performance of SLM-fabricated Ti6Al4V alloy after different stress-relief heat treatments', in Transportation Research Procedia, Elsevier B.V., 2019, pp. 24–29. doi: 10.1016/j.trpro.2019.07.005.
[56] L. B. Malefane, W. B. du Preez, M. Maringa, and A. du Plessis, 'Tensile and high cycle fatigue properties of annealed TI6AL4V (ELI) specimens produced by direct metal laser sintering', South African Journal of Industrial Engineering, vol. 29, no. 3 Special Edition, pp. 299–311, 2018, doi: 10.7166/29-3-2077.
[57] V. Chastand, A. Tezenas, Y. Cadoret, P. Quaegebeur, W. Maia, and E. Charkaluk, 'Fatigue characterization of Titanium Ti-6Al-4V samples produced by Additive Manufacturing', in Procedia Structural Integrity, Elsevier B.V., 2016, pp. 3168–3176. doi: 10.1016/j.prostr.2016.06.395.
[58] S. Leuders et al., 'On the mechanical behaviour of titanium alloy TiAl6V4 manufactured by selective laser melting: Fatigue resistance and crack growth performance', Int J Fatigue, vol. 48, pp. 300–307, 2013, doi: 10.1016/j.ijfatigue.2012.11.011.
[59] M. Tarik Hasib, H. E. Ostergaard, X. Li, and J. J. Kruzic, 'Fatigue crack growth behavior of laser powder bed fusion additive manufactured Ti-6Al-4V: Roles of post heat treatment and build orientation', Int J Fatigue, vol. 142, Jan. 2021, doi: 10.1016/j.ijfatigue.2020.105955.
[60] N. M. Dhansay, T. Hermann Becker, and K. Vanmeensel, 'Fatigue crack growth rate threshold of laser powder bed fusion Ti-6Al-4V', 2021. [Online]. Available: https://scholar.sun.ac.za
[61] H. Clemens, S. Mayer, and C. Scheu, 'Microstructure and Properties of Engineering Materials', in Neutrons and Synchrotron Radiation in Engineering Materials Science: From Fundamentals to Applications: Second Edition, wiley, 2017, pp. 3–20. doi: 10.1002/9783527684489.ch1.
[62] M. Yan and P. Yu, 'An Overview of Densification, Microstructure and Mechanical Property of Additively Manufactured Ti-6Al-4V — Comparison among Selective Laser Melting, Electron Beam Melting, Laser Metal Deposition and Selective Laser Sintering, and with Conventional Powder', in Sintering Techniques of Materials, InTech, 2015. doi: 10.5772/59275.
[63] B. Naab and M. Celikin, 'The role of microstructural evolution on the fatigue behavior of additively manufactured Ti–6Al–4V alloy', Materials Science and Engineering: A, vol. 859, Nov. 2022, doi: 10.1016/j.msea.2022.144232.
[64] R. O. Ritchie, 'Mechanisms of fatigue-crack propagation in ductile and brittle solids', Int J Fract, vol. 100, pp. 55–83, 1999.
[65] A. Sharma, Y. Liu, Q. Nian, and Y. Jiao, 'Data-driven Approach to Predict the Static and Fatigue Properties of Additively Manufactured Ti-6Al-4V', Arizona State University, Tempe, 2020.

[66] M. Motyka, ‘Martensite formation and decomposition during traditional and am processing of two-phase titanium alloys—an overview’, Mar. 01, 2021, MDPI AG. doi: 10.3390/met11030481.
[67] J. Sieniawski, W. Ziaja, K. Kubiak, and M. Motyk, ‘Microstructure and Mechanical Properties of High Strength Two-Phase Titanium Alloys’, in Titanium Alloys - Advances in Properties Control, InTech, 2013. doi: 10.5772/56197.
[68] J. Belan, M. Uhricik, P. Hanusova, and A. Vasko, ‘The Ti6Al4V Alloy Microstructure Modification Via Various Cooling Rates, its Influence on Hardness and Microhardness’, Manufacturing Technology, vol. 20, no. 5, pp. 560–565, 2020, doi: 10.21062/mft.2020.095.
[69] A. L. Pilchak, A. Bhattacharjee, R. E. A. Williams, and J. C. Williams, ‘The Effect of Microstructure on Fatigue Crack Initiation in Ti-6Al-4V’, The Ohio State University, Columbus, 2009.
[70] M. Benedetti and V. Fontanari, ‘The effect of bi-modal and lamellar microstructures of Ti-6Al-4V on the behaviour of fatigue cracks emanating from edge-notches’, Fatigue Fract Eng Mater Struct, vol. 27, no. 11, pp. 1073–1089, Nov. 2004, doi: 10.1111/j.1460-2695.2004.00825.x.
[71] J. Zhao et al., ‘Study on mechanical properties of Ti-6Al-4 V titanium alloy with different microstructures under combined tension-bending load’, J Alloys Compd, vol. 936, Mar. 2023, doi: 10.1016/j.jallcom.2022.168201.
[72] X. Bao, L. Cheng, J. Ding, X. Chen, K. Lu, and W. Cui, ‘The effect of microstructure and axial tension on three-point bending fatigue behavior of TC4 in high cycle and very high cycle regimes’, Materials, vol. 13, no. 1, Jan. 2020, doi: 10.3390/ma13010068.
[73] D. Agius, K. I. Kourousis, and C. Wallbrink, ‘A review of the as-built SLM Ti-6Al-4V mechanical properties towards achieving fatigue resistant designs’, Jan. 19, 2018, MDPI AG. doi: 10.3390/met8010075.
[74] M. Simonelli, Y. Y. Tse, and C. Tuck, ‘Microstructure of Ti-6Al-4V produced by selective laser melting’, in Journal of Physics: Conference Series, Institute of Physics Publishing, 2012. doi: 10.1088/1742-6596/371/1/012084.
[75] P. Zhang, A. N. He, F. Liu, K. Zhang, J. Jiang, and D. Z. Zhang, ‘Evaluation of low cycle fatigue performance of selective laser melted titanium alloy Ti-6Al-4V’, Metals (Basel), vol. 9, no. 10, Oct. 2019, doi: 10.3390/met9101041.
[76] F. Cao, T. Zhang, M. A. Ryder, and D. A. Lados, ‘A Review of the Fatigue Properties of Additively Manufactured Ti-6Al-4V’, JOM, vol. 70, no. 3, pp. 349–357, Mar. 2018, doi: 10.1007/s11837-017-2728-5.
[77] E. Cerri, E. Ghio, and G. Bolelli, ‘Effect of surface roughness and industrial heat treatments on the microstructure and mechanical properties of Ti6Al4V alloy manufactured by laser powder bed fusion in different built orientations’, Materials Science and Engineering: A, vol. 851, Aug. 2022, doi: 10.1016/j.msea.2022.143635.
[78] M. Neikter, ‘Microstructure and texture of additive manufactured Ti-6Al-4V’, Luleå University of Technology, Luleå, 2017.
[79] H. Jaber, J. Kónya, K. Kulcsár, and T. Kovács, ‘Effects of Annealing and Solution Treatments on the Microstructure and Mechanical Properties of Ti6Al4V Manufactured by Selective Laser Melting’, Materials, vol. 15, no. 5, Mar. 2022, doi: 10.3390/ma15051978.
[80] L. Kunz, P. Pokorný, R. Konečná, and G. Nicoletto, ‘Propagation of long fatigue cracks in Ti6Al4V alloy produced by direct metal laser sintering’, in Procedia Structural Integrity, Elsevier B.V., 2019, pp. 222–229. doi: 10.1016/j.prostr.2019.08.030.
[81] T. Yuri, Y. Ono, T. Ogata, and H. Sunakawa, ‘Effect of microstructure on high-cycle fatigue properties of Ti-6Al-4V alloy forging at cryogenic temperatures’, in AIP

Conference Proceedings, American Institute of Physics Inc., 2014, pp. 27–33. doi: 10.1063/1.4860600.

[82] A. H. Chern et al., 'A review on the fatigue behavior of Ti-6Al-4V fabricated by electron beam melting additive manufacturing', Int J Fatigue, vol. 119, pp. 173–184, Feb. 2019, doi: 10.1016/j.ijfatigue.2018.09.022.

[83] P. E. Carrion, N. Shamsaei, S. R. Daniewicz, and R. D. Moser, 'Fatigue behavior of Ti-6Al-4V ELI including mean stress effects', Int J Fatigue, vol. 99, pp. 87–100, Jun. 2017, doi: 10.1016/j.ijfatigue.2017.02.013.

[84] B. Vayssette, N. Saintier, C. Brugger, M. Elmay, and E. Pessard, 'Surface roughness of Ti-6Al-4V parts obtained by SLM and EBM: Effect on the High Cycle Fatigue life', in Procedia Engineering, Elsevier Ltd, 2018, pp. 89–97. doi: 10.1016/j.proeng.2018.02.010.

[85] E. Wycisk, A. Solbach, S. Siddique, D. Herzog, F. Walther, and C. Emmelmann, 'Effects of defects in laser additive manufactured Ti-6Al-4V on fatigue properties', in Physics Procedia, Elsevier B.V., 2014, pp. 371–378. doi: 10.1016/j.phpro.2014.08.120.

[86] B. Fotovvati, N. Namdari, and A. Dehghanghadikolaei, 'Fatigue performance of selective laser melted Ti6Al4V components: State of the art', Mater Res Express, vol. 6, no. 1, Jan. 2019, doi: 10.1088/2053-1591/aae10e.

[87] W. Eric, E. Claus, S. Shafaqat, and W. Frank, 'High cycle fatigue (HCF) performance of Ti-6Al-4V alloy processed by selective laser melting', in Advanced Materials Research, 2013, pp. 134–139. doi: 10.4028/www.scientific.net/AMR.816-817.134.

[88] A. E. Patterson, S. L. Messimer, and P. A. Farrington, 'Overhanging Features and the SLM/DMLS Residual Stresses Problem: Review and Future Research Need', Technologies (Basel), vol. 5, no. 4, p. 15, Apr. 2017, doi: 10.3390/technologies5020015.

[89] W. H. Kan et al., 'A critical review on the effects of process-induced porosity on the mechanical properties of alloys fabricated by laser powder bed fusion', Jun. 01, 2022, Springer. doi: 10.1007/s10853-022-06990-7.

[90] M. G. Moletsane, P. Krakhmalev, N. Kazantseva, A. du Plessis, I. Yadroitsava, and I. Yadroitsev, 'Tensile properties and microstructure of direct metal laser-sintered Ti6Al4V (ELI) alloy', South African Journal of Industrial Engineering, vol. 27, no. 3SpecialIssue, pp. 110–121, 2016, doi: 10.7166/27-3-1667.

[91] A. Guzanová, G. Ižaríková, J. Brezinová, J. Živčák, D. Draganovská, and R. Hudák, 'Influence of build orientation, heat treatment, and laser power on the hardness of Ti6Al4V manufactured using the DMLS process', Metals (Basel), vol. 7, no. 8, Aug. 2017, doi: 10.3390/met7080318.

[92] M. G. Moletsane, 'Microstructure and mechanical properties of Ti6Al4V (ELI) parts produced by DMLS', Master Technology, Central University of Technology, Free State, Bloemfontein, 2016.

[93] V. D. Le, E. Pessard, F. Morel, and S. Prigent, 'Fatigue behaviour of additively manufactured Ti-6Al-4V alloy: The role of defects on scatter and statistical size effect', Int J Fatigue, vol. 140, Nov. 2020, doi: 10.1016/j.ijfatigue.2020.105811.

[94] D. Wang et al., 'Densification, Tailored Microstructure, and Mechanical Properties of Selective Laser Melted Ti–6Al–4V Alloy via Annealing Heat Treatment', Micromachines (Basel), vol. 13, no. 2, Feb. 2022, doi: 10.3390/mi13020331.

[95] ASTM International, ' Standard Terminology for Additive Manufacturing—Coordinate Systems and Test Methodologies', Ohio, 2013.

[96] M. Rybachuk, C. Alice Mauger, T. Fiedler, and A. Öchsner, 'Anisotropic mechanical properties of fused deposition modeled parts fabricated by using acrylonitrile butadiene styrene polymer', Journal of Polymer Engineering, vol. 37, no. 7, pp. 699–706, Sep. 2017, doi: 10.1515/polyeng-2016-0263.

[97] A. Bača, R. Konečná, G. Nicoletto, and L. Kunz, 'Influence of Build Direction on the Fatigue Behaviour of Ti6Al4V Alloy Produced by Direct Metal Laser Sintering', in

Materials Today: Proceedings, Elsevier Ltd, 2016, pp. 921–924. doi: 10.1016/j.matpr.2016.03.021.

[98] C. R. Knowles, T. H. Becker, and R. B. Tait, 'RESIDUAL STRESS MEASUREMENTS AND STRUCTURAL INTEGRITY IMPLICATIONS FOR SELECTIVE LASER MELTED TI-6AL-4V #', South African Journal of Industrial Engineering, vol. 23, no. 3, 2012.

[99] L. B. Malefane, 'Determination of the Fatigue Properties of Ti6Al4V (ELI) Parts built by a Direct Metal Laser Sintering System with Standard Process Parameters Followed by Post-Processing Treatments', Master of Engineering, Central University of Technology, Free State, Bloemfontein, 2019.

[100] Q. C. Liu, J. Elambasseril, S. J. Sun, M. Leary, M. Brandt, and P. K. Sharp, 'The effect of manufacturing defects on the fatigue behaviour of Ti-6Al-4V specimens fabricated using selective laser melting', in Advanced Materials Research, Trans Tech Publications, 2014, pp. 1519–1524. doi: 10.4028/www.scientific.net/AMR.891-892.1519.

[101] K. S. Chan, M. Koike, R. L. Mason, and T. Okabe, 'Fatigue life of titanium alloys fabricated by additive layer manufacturing techniques for dental implants', Metall Mater Trans A Phys Metall Mater Sci, vol. 44, no. 2, pp. 1010–1022, Feb. 2013, doi: 10.1007/s11661-012-1470-4.

[102] G. M. Ter Haar and T. H. Becker, 'Low temperature stress relief and martensitic decomposition in selective laser melting produced Ti6Al4V', Material Design and Processing Communications, vol. 3, no. 1, Feb. 2021, doi: 10.1002/mdp2.138.

[103] V. Cain, L. Thijs, J. Van Humbeeck, B. Van Hooreweder, and R. Knutsen, 'Crack propagation and fracture toughness of Ti6Al4V alloy produced by selective laser melting', Addit Manuf, vol. 5, pp. 68–76, Jan. 2015, doi: 10.1016/j.addma.2014.12.006.

[104] Z. W. Xu, A. Liu, and X. S. Wang, 'The influence of building direction on the fatigue crack propagation behavior of Ti6Al4V alloy produced by selective laser melting', Materials Science and Engineering: A, vol. 767, Nov. 2019, doi: 10.1016/j.msea.2019.138409.

[105] S. Kumar, K. Chattopadhyay, and V. Singh, 'Tensile Behavior of Ti-6Al-4V alloy at Elevated Temperatures', 2014. [Online]. Available: https://www.researchgate.net/publication/308787239

[106] S. Ivanov, M. Gushchina, A. Artinov, M. Khomutov, and E. Zemlyakov, 'Effect of Elevated Temperatures on the Mechanical Properties of a Direct Laser Deposited Ti-6Al-4V', Materials, vol. 14, no. 21, 2021, doi: 10.3390/ma.

[107] R. Liu, Y. Tian, Z. Zhang, X. An, P. Zhang, and Z. Zhang, 'Exceptional high fatigue strength in Cu-15at.%Al alloy with moderate grain size', Sci Rep, vol. 6, Jun. 2016, doi: 10.1038/srep27433.